Decay of nuclear hyperpolarization in silicon microparticles

M. Lee,[1] M. C. Cassidy,[2] C. Ramanathan,[3] and C. M. Marcus[1,*]

[1]*Department of Physics, Harvard University, Cambridge, Massachusetts 02138, USA*
[2]*School of Engineering and Applied Sciences, Harvard University, Cambridge, Massachusetts 02138, USA*
[3]*Department of Physics and Astronomy, Dartmouth College, Hanover, New Hampshire 03755, USA*

We investigate the low-field relaxation of nuclear hyperpolarization in undoped and highly doped silicon microparticles at room temperature following removal from high field. For nominally undoped particles, two relaxation time scales are identified for ambient fields above 0.2 mT. The slower, $T_{1,\mathrm{s}}$, is roughly independent of ambient field; the faster, $T_{1,\mathrm{f}}$, decreases with increasing ambient field. A model in which nuclear spin relaxation occurs at the particle surface via a two-electron mechanism is shown to be in good agreement with the experimental data, particularly the field independence of $T_{1,\mathrm{s}}$. For boron-doped particles, a single relaxation time scale is observed. This suggests that for doped particles, mobile carriers and bulk ionized acceptor sites, rather than paramagnetic surface states, are the dominant relaxation mechanisms. Relaxation times for the undoped particles are not affected by tumbling in a liquid solution.

PACS number(s): 76.60.−k, 87.85.Rs, 82.56.Lz, 87.61.−c

I. INTRODUCTION

Silicon has long been a staple of the microelectronics industry and so has been the subject of intense materials research. In recent years, nanoscale silicon has attracted attention due to its unique electronic and optical properties,[1–3] and as a potential agent for medical imaging and drug delivery.[4–6] Spin phenomena in silicon have been investigated using nuclear magnetic resonance (NMR) for over a half century,[7–14] while material properties and fabrication have continually developed. For instance, the nuclear spin-lattice relaxation time, T_1, provides information about dopants and impurities.[11–13] Notably, the low natural abundance (4.7%) of spin-1/2 ^{29}Si nuclei in a lattice of zero spin nuclei leads to T_1 of many hours[6,13] and coherence times up to tens of seconds[14] in undoped bulk crystalline silicon.

These remarkable NMR properties have stimulated interest in silicon as a platform for solid-state quantum computing[15–17] and as a long-lived imaging agent for hyperpolarized magnetic resonance imaging (MRI).[6] In particular, there have been renewed efforts to understand dynamic nuclear polarization (DNP), a process where saturation or pumping of paramagnetic impurity states by microwave fields or optical illumination can lead to nuclear spin polarizations orders of magnitude larger than thermal equilibrium polarizations.[18–22] Enhancing polarization by these methods is commonly referred to as hyperpolarization.

Application of silicon as a hyperpolarized imaging agent for MRI requires an understanding of nuclear spin relaxation over a broad range of applied fields, from high fields where polarization is induced and imaged, to low fields where the agent is transferred from the polarizer and administered. Previous detailed studies have focused on low temperatures, investigating the dependence of T_1 on applied magnetic field, doping,[23–25] and strain.[26] It was found that T_1 increased with applied magnetic field, which was explained in terms of the field dependence of electron-nuclear dipole-dipole interaction. The nuclear T_1 was also shown to scale inversely with the concentration of mobile carriers.[12,13] In silicon nanoparticles, the observed increase in nuclear T_1 with increasing particle size

was attributed to diffusion-mediated relaxation via defects at the particle surface.[6] Recent measurements have shown that the relaxation and coherence times of ^{31}P donor-bound electron spin are dramatically reduced near the silicon surface due to P_b defects, in comparison to known values in the bulk.[27] Studies of electrically[9] and optically[10] detected hyperpolarization of ^{31}P donor nuclear spins near the silicon surface, however, do not consider effects of the surface on nuclear spin relaxation.

In this paper, we investigate the decay of hyperpolarization of ^{29}Si nuclei in silicon microparticles at room temperature and low ambient magnetic fields. The hyperpolarization for this experiment was induced by waiting for nuclear spins to fully relax to thermal equilibrium in a high-field, room temperature polarizing environment, prior to the placement of sample in the low-field depolarizing environment. Thus the sample was kept at room temperature at all times, ensuring that the applied magnetic field, not sample temperature, was responsible for all measured effects on low-field nuclear spin relaxation that are reported here.

We find the decay is bi-exponential, with a slow time scale that is independent of ambient field, and a fast time scale that shows only a modest decrease with increasing ambient field. We develop a model of nuclear spin relaxation in silicon particles that takes into account the heterogeneous makeup of the sample, with direct nuclear relaxation occurring only near the surface, while nuclei in the particle core are relaxed indirectly by spin diffusion. This model extends a previous spin diffusion model,[18] which predicts T_1 increasing with the square of the particle diameter. We find that the weak magnetic field dependence observed experimentally is inconsistent with a simple extended spin-diffusion model based on relaxation of individual bound electrons. However, by generalizing the model further to include nuclear spin relaxation mediated by pairs of dipolar-coupled electrons, the essentially field-independent relaxation is recovered by the model.[30,33–35] The experimental methods presented here, as well as the use of magnetic field dependence of nuclear T_1 as a probe for testing the relative importance of these different model processes, have precedent in a similar investigation performed on diamond and its ^{13}C nuclear spin relaxation.[30–32]

II. SAMPLES AND MEASUREMENTS

Microparticles made from nominally undoped and boron-doped ball-milled Si wafers were investigated. As shown previously,[6] undoped Si microparticles have very long high-field relaxation times ($T_1 \sim 10^4$ s), relevant for hyperpolarized MRI. Undoped samples were produced by ball-milling high-resistivity (>10 kΩ·cm) float-zone Si wafers (Silicon Quest International) followed by size separation by centrifugal sedimentation, yielding a mean particle diameter of 5 μm.[6] Boron-doped Si microparticles with doping density $\sim 5 \times 10^{18}$ cm^{-3} have much faster nuclear spin relaxation, $T_1 \sim 10^2$ s at high magnetic field. The boron-doped microparticles were produced by ball-milling Czochralski-grown Si wafers (Virginia Semiconductor, resistivity 0.01–0.02 Ω·cm) followed by size separation, yielding a mean particle diameter on the order of 10 μm. Except where noted, samples consisted of a 0.1 mL teflon tube filled with particles. All NMR measurements were carried out at $B_0 = 2.9$ T using a custom-built probe and spectrometer.

Polarization at 2.9 T following a saturation sequence of sixteen $\pi/2$ pulses was measured as a function of time, t_{pol}, using a Carr-Purcell-Meiboom-Gill (CPMG) sequence,[36–38] $(\pi/2)_X - [t/2 - (\pi)_Y - t/2 - \text{echo}]^n$ with $t = 1$ ms and $n = 400$. After each data point, the sample was re-saturated and the measurement repeated. As seen in Figs. 1(a) and 4(a), the buildup of polarization is well described by a single exponential function of t_{pol} for both undoped and doped samples.
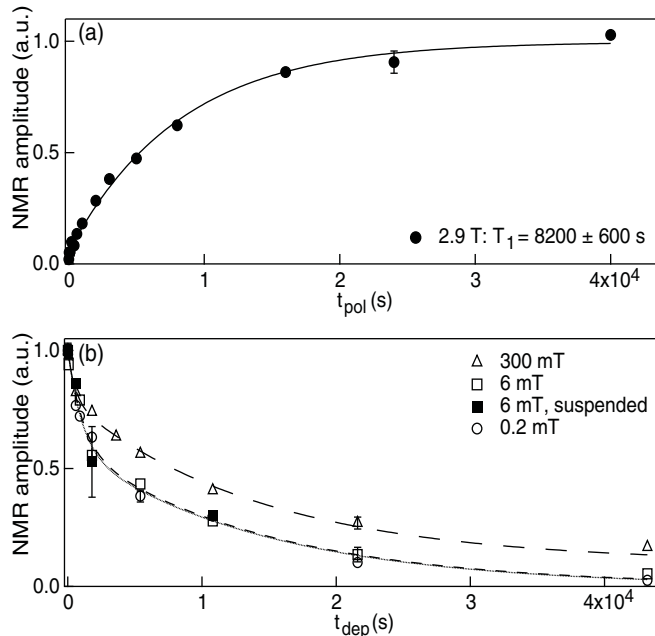

FIG. 1. Relaxation of nuclear spin polarization of undoped silicon particles. (a) Recovery of spin polarization following saturation at $B_0 = 2.9$ T. (b) Decay of nuclear magnetization at $B_{\text{dep}} = 0.2$ mT (circles), 6 mT (open squares), and 300 mT (triangles), after polarization at 2.9 T, and same data for particles suspended in methanol at 6 mT (filled squares). Curves show best fits to Eq. (1). No signal was observed after 1 second in the zero-field chamber (<1 μT).

Depolarization at low ambient fields was measured after first polarizing at 2.9 T for 8 h ($\sim 3 T_1$ at 2.9 T), then raising the probe out of the magnet bore to a position where ambient (or holding) fields of 0.2 mT, 6 mT, 130 mT, and 300 mT had been previously calibrated using a Lakeshore 460 gaussmeter. In addition, a nominal zero-field measurement used a commercial zero-gauss chamber (Lakeshore 4060) with ambient field below 1 μT. Following depolarization in ambient field, the sample was returned to field center (2.9 T) and the remaining nuclear polarization was measured using the CPMG sequence described above. The transit time between positions was ~ 5 s, fast compared to T_1 but slow compared to nuclear Larmor times. The sample was fully repolarized following each data point.

In addition to NMR measurements, room-temperature electron spin resonance (ESR) measurements were carried out to characterize electronic defects and carriers of the two sample types. The ESR spectrum of the undoped sample showed a single peak at $B = 324$ mT measured at ESR frequency $f = 9.099$ GHz, corresponding to a g factor centered at 2.006, with a linewidth of 0.47 mT. The ESR spectrum of the boron-doped sample showed a single peak at $B = 336$ mT measured at ESR frequency $f = 9.444$ GHz, again corresponding to a g factor of 2.006. A g factor of 2.006 is consistent with reported values for P_b defects at the Si/SiO$_2$ interface, and is not consistent with g factors of other common dopants or oxide states.[39,40]

For each sample, an estimate of the electron spin concentration on the particle surface was made by taking ESR spectra with a piece of phosphorus-doped silicon wafer (0.01–0.1 Ω·cm) also inserted in the spectrometer cavity. The addition of the wafer piece resulted in the appearance of additional ESR signal due to the n-type doping. Comparing the peak areas and using the known doping level of the wafer piece yielded an order-of-magnitude estimate of the mean volume density of defect spins, which was $\sim 10^{18}$ cm^{-3} in both samples. Assuming a surface-to-volume ratio of 300 nm-radius spheres, this mean volume density corresponds to a surface defect concentration of 10^{13} cm^{-2}. Transmission electron micrographs reveal an oxide layer of 2–3 nm at the surface of the ball-milled particle. The relevant P_b defects reside at the interface between the crystalline Si and this oxide layer.

A. Undoped microparticles: measurements

Polarization and depolarization data for the undoped microparticles are shown in Fig. 1. Polarization is well described by a simple exponential, $P = P_{0,B_0}(1 - e^{-t_{\text{pol}}/T_1})$, with best-fit value $T_1 = 8200 \pm 600$ s, consistent with previous measurements.[6] Equilibrium polarization is small, $P_{0,B_0} = \tanh[(\hbar \gamma_n B_0)/(2k_B T)] = 2 \times 10^{-6}$. Here, k_B is the Boltzmann constant, $T = 300$ K is room temperature, and $\gamma_n = 5.31 \times 10^7$ s^{-1} T^{-1} is the nuclear gyromagnetic ratio for ^{29}Si.

In contrast to the buildup of polarization at 2.9 T, depolarization at low ambient fields, B_{dep}, decays with two distinct time scales, which we characterize using a bi-exponential form,

$$P = P_{0,B_{\text{dep}}} + (P_{0,B_0} - P_{0,B_{\text{dep}}})$$
$$\times [(1 - \alpha)e^{-t_{\text{dep}}/T_{1,\text{f}}} + \alpha e^{-t_{\text{dep}}/T_{1,\text{s}}}], \quad (1)$$

TABLE I. Exponential weights and relaxation times fitting to experimental data. $T_{1,\text{f}}$ and $T_{1,\text{s}}$ are fast and slow relaxation times with which two additive components of the spin polarization decay. α is the relative amplitude of the component which decays at $T_{1,\text{s}}$.

B_{dep}	α	$T_{1,\text{f}}$ (s)	$T_{1,\text{s}}$ (s)
300 mT	0.765 ± 0.027	531 ± 179	13850 ± 1030
6 mT	0.593 ± 0.050	903 ± 232	15310 ± 2070
0.2 mT	0.591 ± 0.120	1124 ± 544	14910 ± 5360
<1 μT		<1	

where $T_{1,\text{f}}$ and $T_{1,\text{s}}$ are fast and slow relaxation times, and α is the fraction of spins whose polarization decays slowly. Best-fit values of α, $T_{1,\text{f}}$, and $T_{1,\text{s}}$ are shown in Table I. Note that the slow relaxation time depends very weakly on B_{dep}, with $T_{1,\text{s}} \sim (1.4$–$1.5) \times 10^3$ s in all cases. In contrast, fast relaxation becomes somewhat faster (shorter $T_{1,\text{f}}$) with increasing B_{dep}, while the fraction of slow relaxers increases.

Inside the zero-gauss chamber the residual ambient magnetic field is specified to be below the few-μT scale, much weaker than the typical nuclear dipolar field, $B_{n,dd} \sim \mu_0 \mu_n/(4\pi a^3) = 0.08$ mT, where $a \sim 4$ Å is the mean separation between randomly distributed ^{29}Si nuclei. At such extremely low fields, spin transitions will occur that are forbidden when $B > B_n$ by the conservation of nuclear Zeeman energy, and nuclear spin relaxation is as fast as decoherence.[41] As expected, we find that in the zero-gauss chamber nuclear polarization decays very quickly, with no visible signal for $t_{\text{dep}} > 1$ s.

To investigate the effect of microparticle tumbling on depolarization, a fluid mixture of one part Si microparticles and four parts methanol by weight was compared to a sample of packed dry powder. Depolarization times at 6 mT ambient field showed no significant difference in relaxation times.

B. Undoped microparticles: model

We interpret NMR and ESR data for the undoped microparticles within a model shown schematically in Fig. 2, comprising nuclear dipolar diffusion in a core region and relaxation via paramagnetic sites in a shell region near the Si/SiO$_2$ interface. In undoped silicon, direct coupling of ^{29}Si nuclear spins to phonons is weak,[11,33] and dipolar coupling to paramagnetic impurities and defects typically dominates nuclear spin relaxation. Within our model, the bi-exponential form of Eq. (1) reflects the existence of two populations of nuclear spins within each microparticle: A fraction α, located in the core of the particle, has a long spin relaxation time $T_{1,\text{s}}$ mediated by nuclear spin diffusion; the remaining fraction $(1 - \alpha)$, located within a shell near the Si/SiO$_2$ interface, has a short relaxation time $T_{1,\text{f}}$ mediated by electron-nuclear-spin interaction associated with paramagnetic centers at the Si/SiO$_2$ interface.

For $B_{\text{dep}} > B_{n,dd}$, the nuclear dipolar spin diffusion rate is independent of magnetic field[22] and is well described by a diffusion constant $D = Wa^2 \sim a^2/(50\,T_2)$, where W is the probability of a flip-flop transition between nuclei due to dipole-dipole interaction, and T_2 is the nuclear decoherence
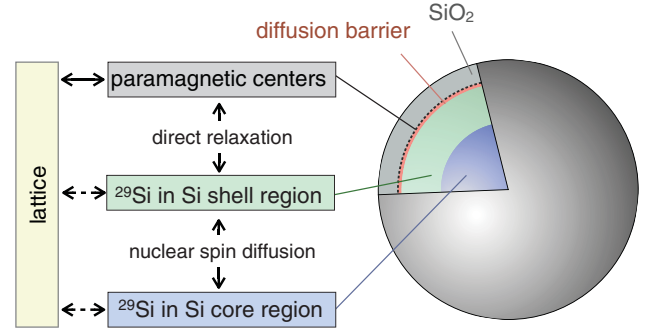

FIG. 2. (Color online) Model showing the spin reservoirs and relaxation pathways in undoped silicon particles. Nuclei in the core region of the particle relax by transferring their magnetization to the nuclei in the shell region, nearer to the surface, by spin diffusion. The nuclei near the surface can relax quickly due to strong dipolar coupling to paramagnetic defects at the Si/SiO$_2$ interface.

time.[33] This is consistent with our observation that $T_{1,\text{s}}$ is roughly independent of B_{dep} across a broad range of values.

The thickness of the shell region is set by the nuclear spin diffusion radius, $\beta = (C/D)^{1/4}$, where C is a constant describing the nature of the dipolar interaction occurring between the nuclei and electrons. Nuclei situated at a distance r from the electrons at the particle surface may relax through a dipolar interaction with the electrons at a rate $\propto C/r^6$.[33]

We consider two physical mechanisms of relaxation in the shell region, one in which each nuclear spin interacts with a single electron spin, and the other in which each nuclear spin interacts with a pair of electron spins. The two-electron model captures a crucial physical mechanism by allowing energy matching between electron-spin-pair flip-flops and nuclear spin flips in a magnetic field, leading to efficient nuclear relaxation with weak dependence on magnetic field.

Modeling nuclear spin relaxation as arising from interaction with individual paramagnetic centers is appropriate for sparsely distributed impurities. This regime has been studied experimentally, for instance, in diamagnetic crystals such as LiF[42,43] and CaF$_2$.[44] In this case, the orientation-averaged dipole interaction strength is given by

$$C_{(1e)} = \frac{3}{10} \frac{\hbar^2 \gamma_e^2}{T_{1e} B_{\text{dep}}^2},\qquad(2)$$

where γ_e is the gyromagnetic ratio of the electron and T_{1e} the electron spin-lattice relaxation time.[33] This model yields a magnetic field dependence of diffusion-limited relaxation ($R \gg \beta$) at least as strong as $T_{1,\text{s}} \propto B_{\text{dep}}^{1/2}$ because the diffusion radius β and relaxation rate $\propto C$ depend explicitly on field, even when D is field independent.[33,44,45] This prediction is incompatible with our experimental results, which show a much weaker field dependence.

In light of this inconsistency, we consider a model of nuclear relaxation at the particle surface that includes three-spin processes involving pairs of interacting electrons, which gives

$$C_{(2e)} = \frac{3}{10} \frac{\hbar^2 \gamma_e^2}{B_{\text{dep}}^2} \frac{B_{\text{dep}}^2 \gamma_n^2 T_{2e}}{1 + B_{\text{dep}}^2 \gamma_n^2 T_{2e}^2} \int_{-\infty}^{\infty} \frac{g(\omega)g(\omega - \omega_n)}{g(0)} \, d\omega,\qquad(3)$$

where T_{2e} is the electron spin-spin coupling and $g(\omega)$ is the normalized electron absorption line-shape function.[30,34] This model has been previously applied to systems with more concentrated paramagnetic impurities, including $La_2Mg_3(NO_3)_{12} \cdot 24H_2O$[46,47] and more recently ^{13}C nuclear spin relaxation in diamond.[30,31] This model accounts for flip-flop transitions between nearby electron pairs, occurring on a time scale $T_{2e} \ll T_{1e}$, which provide the fluctuating magnetic field that can flip nuclear spins. That is, when the dipolar coupling of electron pairs matches the nuclear Zeeman energy, a three-spin interaction can occur that exchanges the spins of the two electrons while flipping a nuclear spin.[48] This process depends on the density of transitions between electronic dipolar energy states that match the nuclear Zeeman energy. For a Lorentzian electron line shape, the integral in (3), which describes the probability of finding two electrons within the ESR line differing in frequency by ω_n, can be replaced by $2/(4 + \omega_n^2 T_{2e}^2)$. For low B_{dep}, such that $\gamma_n B_{\mathrm{dep}} < \gamma_e B_{e,dd} \sim T_{2e}^{-1}$, where $B_{e,dd}$ is the electronic dipolar field, the density of nuclear-spin-flip transitions will be independent of B_{dep}, hence the rate of direct nuclear spin relaxation by this process will also be independent of B_{dep}.[30,34]

We infer an upper bound for $B_{e,dd}$ from the measured ESR linewidth of 0.47 mT, which gives $\gamma_n^{-1}\gamma_e B_{e,dd} \sim 1.7$ T for the scale of B_{dep} below which nuclear T_1 should be roughly field independent within this three-spin model. The low end of the field-independent range is set by the nuclear dipolar field $B_{n,dd} \sim 0.08$ mT. This range is consistent with the experimental observation that $T_{1,s}$ is roughly field independent from 0.2 mT to 300 mT. Weak field dependencies of $T_{1,f}$ and α are likely due to the weak field dependence of T_{1e}.

Very close to each paramagnetic impurity, nuclear spin diffusion is suppressed, creating a barrier to diffusion of radius $b = a(\hbar \gamma_e^2 B_{\mathrm{dep}}/\gamma_n 2k_B T)^{1/4}$, due to gradients in the nuclear Larmor frequency.[33] This effect is included in the simulations (described below), but because $\beta \gg b$ it only weakly affects overall relaxation times.

We have simulated nuclear spin relaxation as a function of ambient field for a spherical silicon microparticle with native ^{29}Si concentration and paramagnetic sites at the surface. For both one and two electron processes, the average polarization $P(t_{\mathrm{dep}})$ is approximately bi-exponential, similar to the experimental data. Fits to the relaxation curves gave $T_{1,s}$ and $T_{1,f}$ values shown in Fig. 3. The particle diameter was taken to be 700 nm, smaller than the actual mean particle size. This compensated the spherical assumption, which gave too small of a surface where defects reside. Other parameters in the model were nuclear T_2 of 10 ms (and corresponding nuclear spin diffusion constant 0.3 nm^2/s), electron T_{1e} of 200 ns, and electron T_{2e} of 25 ns. Figure 3 shows the striking contrast in field dependence between the two models, and that the three-spin process compares relatively well with experiment.

C. Results for boron-doped microparticles

Nuclear polarization and depolarization of boron-doped Si microparticles are shown in Fig. 4. Both $P(t_{\mathrm{pol}})$ and $P(t_{\mathrm{dep}})$ are well fitted by single-exponential relaxation curves with time constants T_1 that increase with increasing ambient field. The reduction of T_1 by 1–2 orders of magnitude in the doped case reflects the dominant contribution of nuclear relaxation from mobile carriers,[12] as well as from non-ionized dopants distributed uniformly through the particle instead of just at the surface (Fig. 5), both bypassing the relatively slow nuclear spin diffusion process. The measured T_1 in the microparticles is consistent with previous reports of the nuclear relaxation rate due to mobile holes in bulk p-type silicon doped to similar concentrations,[13] and we therefore conclude that the dominant

FIG. 4. Nuclear spin lattice relaxation in boron-doped silicon microparticles. (a) Recovery of spin polarization after saturation at $B_0 = 2.9$ T. (b) Decay of nuclear magnetization at $B_{\mathrm{dep}} = 6$ mT (open squares) and 130 mT (triangles), after polarization at 2.9 T. Error bars in (a) are displayed but smaller than the data points shown.
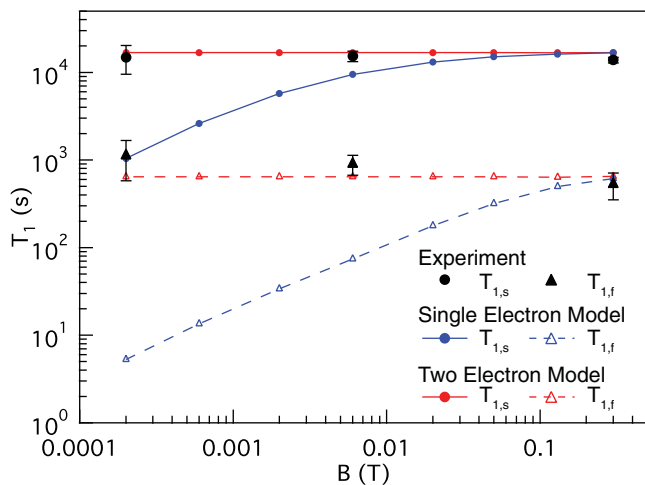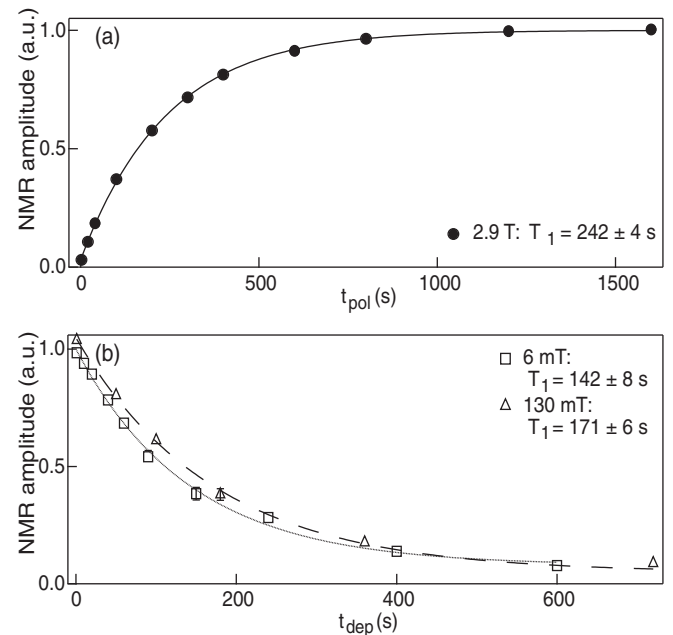

FIG. 3. (Color online) Experimental slow (black circles) and fast (black triangles) relaxation times, $T_{1,s}$ and $T_{1,f}$, from Table I, for bi-exponential nuclear spin relaxation, along with simulation results for a model that includes either one-electron or two-electron processes.
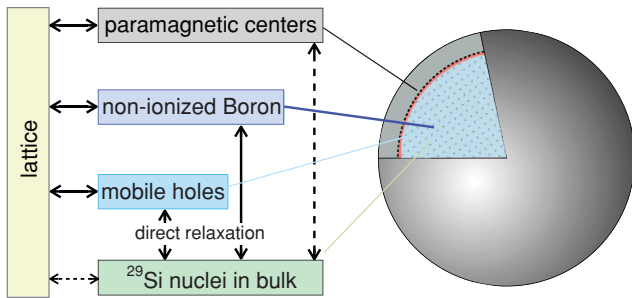
FIG. 5. (Color online) Rate model showing dominant nuclear relaxation pathways of direct relaxation on mobile holes and short diffusion to non-ionized B (i.e., bound holes) throughout the bulk of the particle. Long-distance spin diffusion to surface impurities is relatively slow and direct coupling of the nuclei to the lattice is weak.

nuclear relaxation mechanisms are the same as in these bulk systems.

The contribution of non-ionized dopants and mobile carriers can be expressed as an additional relaxation rate that is proportional to the relative strength of each interaction weighted by the relative fractions of ionized and non-ionized dopants ($\sim$5% ionized at room temperature). For free carriers this interaction is independent of magnetic field,[12] while for non-ionized dopants a magnetic field dependence will be present due to the paramagnetic nature of the bound hole. However, this dependence will be small due to the high doping concentration of the sample. For the specified dopant density, the average distance between dopants is $\sim$2.5 nm and the Bohr radius $\sim$1.3 nm,[49] both an order of magnitude less than the diffusion radius for both single-electron and two-electron processes across the range of ambient fields under study. It is likely that this is the source of the small magnetic field dependence seen in Fig. 4(b).

III. CONCLUSION

We have investigated the relaxation of polarization of natural-abundance ^{29}Si nuclei in undoped and doped silicon microparticle samples as a function of ambient magnetic fields at room temperature. In undoped micron-scale particles, the decay of nuclear polarization from a hyperpolarized value was measured from microtesla to 0.3 T. For fields stronger

than the nuclear dipolar field, a bi-exponential decay of nuclear magnetization was observed, with a fast component of $\sim$$10^2$ s that depends weakly on field and a slow component of $\sim$$10^4$ s that is roughly field independent. The relative amplitude of the slowly decaying component increases with the magnetic field, but only slightly. Bi-exponential relaxation suggests the presence of two nuclear spin baths distinguished by their proximity to paramagnetic impurities at the particle surface. The time scales of nuclear spin relaxation are largely independent of ambient field B_{dep} from 0.2 to 300 mT. This independence from B_{dep} is quantitatively consistent with a model of nuclear spin relaxation dominated by a three-spin mechanism in which flip-flop transitions of two electrons at the nuclear Larmor frequency flip a nuclear spin. In highly doped silicon, simple exponential relaxation with a faster T_1 of order a few hundred seconds is observed.

These results can be compared with similar experiments performed in diamond, another material with dilute (1.1%) spin-1/2 nuclei among a majority of zero-spin nuclei in an fcc lattice.[28–30] Measurements of the nuclear T_1 in natural diamond as a function of magnetic field indicate a contribution of three-spin processes to ^{13}C spin relaxation.[30] Other investigations of nuclear spin relaxation in ^{13}C-enriched diamond[31] and in nanocrystalline diamond[32] have shown that the relaxation of nuclear magnetization was not well described by a simple exponential approach to equilibrium. The NMR studies in nanocrystalline diamond revealed that the particles consist of a crystalline core and a surrounding shell. All these observations in diamond are similar to our results in silicon microparticles.

Finally, we comment that multihour and field-independent nuclear relaxation times for a substantial fraction of the nuclear spin population, including for particles in a fluid suspension, are important for the use of silicon microparticles as a hyperpolarized MRI imaging agent.

*marcus@harvard.edu

[1]G. Ledoux, J. Gong, F. Huisken, O. Guillois, and C. Reynaud, Appl. Phys. Lett. **80**, 4834 (2002).

[2]B. Delley and E. F. Steigmeier, Appl. Phys. Lett. **67**, 2370 (1995).

[3]T. Y. Kim, N. M. Park, K. H. Kim, G. Y. Sung, Y. W. Ok, T. Y. Seong, and C. J. Choi, Appl. Phys. Lett. **85**, 5355 (2004).

[4]E. Tasciotti, X. Liu, R. Bhavane, K. Plant, A. D. Leonard, B. K. Price, M. M. Cheng, P. Decuzzi, J. M. Tour, F. Robertson, and M. Ferrari, Nature Nanotechnology **3**, 151 (2008).

[5]J. H. Park, L. Gu, G. von Maltzahn, E. Ruoslahti, S. N. Bhatia, and M. J. Sailor, Nature Mater. **8**, 331 (2009).

[6]J. W. Aptekar *et al.*, ACS Nano **3**, 4003 (2009).

[7]D. Pines, J. Bardeen, and C. P. Slichter, Phys. Rev. **106**, 489 (1957).

[8]G. Feher, Phys. Rev. Lett. **3**, 135 (1959).

[9]D. R. McCamey, J. van Tol, G. W. Morley, and C. Boehme, Phys. Rev. Lett. **102**, 027601 (2009).

[10]A. Yang, M. Steger, T. Sekiguchi, M. L. W. Thewalt, T. D. Ladd, K. M. Itoh, H. Riemann, N. V. Abrosimov, P. Becker, and H. J. Pohl, Phys. Rev. Lett. **102**, 257401 (2009).

[11]N. Bloembergen, Physica **15**, 386 (1949).

[12]N. Bloembergen, Physica **20**, 1130 (1954).

[13] R. G. Shulman and B. J. Wyluda, Phys. Rev. **103**, 1127 (1956).

[14] T. D. Ladd, D. Maryenko, Y. Yamamoto, E. Abe, and K. M. Itoh, Phys. Rev. B **71**, 014401 (2005).

[15] B. E. Kane, Nature (London) **393**, 133 (1998).

[16] T. D. Ladd, J. R. Goldman, F. Yamaguchi, Y. Yamamoto, E. Abe, and K. M. Itoh, Phys. Rev. Lett. **89**, 017901 (2002).

[17] K. Itoh, Solid State Commun. **133**, 747 (2005).

[18] A. E. Dementyev, D. G. Cory, and C. Ramanathan, Phys. Rev. Lett. **100**, 127601 (2008).

[19] A. S. Verhulst, I. G. Rau, Y. Yamamoto, and K. M. Itoh, Phys. Rev. B **71**, 235206 (2005).

[20] H. Hayashi, T. Itahashi, K. M. Itoh, L. S. Vlasenko, and M. P. Vlasenko, Phys. Rev. B **80**, 045201 (2009).

[21] G. Lampel, Phys. Rev. Lett. **20**, 491 (1968).

[22] A. Abragam, J. Combrisson, and I. Solomon, Comptes Rendus **246**, 1035 (1958).

[23] N. T. Bagraev, E. P. Bochkarev, L. S. Vlasenko, V. P. Grishin, and Yu. A. Karpov, Sov. Phys. Solid State **21**, 305 (1979).

[24] N. T. Bagraev, L. S. Vlasenko, and R. A. Zhitnikov, Sov. Phys. Solid State **24**, 1972 (1982).

[25] N. T. Bagraev, L. S. Vlasenko, and R. A. Zhitnikov, Sov. Phys. JETP **49**, 278 (1979).

[26] N. T. Bagraev and L. S. Vlasenko, Sov. Phys. Solid State **24**, 1974 (1982).

[27] S. Y. Paik, S. Y. Lee, W. J. Baker, D. R. McCamey, and C. Boehme, Phys. Rev. B **81**, 075214 (2010).

[28] M. J. R. Hoch and E. C. Reynhardt, Phys. Rev. B **37**, 9222 (1988).

[29] E. C. Reynhardt and C. J. Terblanche, Chem. Phys. Lett. **269**, 464 (1997).

[30] C. J. Terblanche, E. C. Reynhardt, S. A. Rakitianskia, and J. A. Van Wyk, Solid State Nucl. Magn. Reson. **19**, 107 (2001).

[31] E. Shabanova, K. Schaumburg, and J. P. F. Sellschop, J. Magn. Reson. **130**, 8 (1998).

[32] A. M. Panich, A. I. Shames, H. M. Vieth, E. Osawa, M. Takahashi, and A. Ya. Vul', Eur. Phys. J. B **52**, 397 (2006).

[33] G. R. Khutsishvili, Sov. Phys. Usp. **8**, 743 (1966).

[34] M. J. Duijvestijn, R. A. Wind, and J. Smidt, Physica B + C **138**, 147 (1986).

[35] C. Ramanathan, Appl. Magn. Reson. **34**, 409 (2008).

[36] H. Y. Carr and E. M. Purcell, Phys. Rev. **94**, 630 (1954).

[37] S. Meiboom and D. Gill, Rev. Sci. Instrum. **29**, 6881 (1958).

[38] D. Li, Y. Dong, R. G. Ramos, J. D. Murray, K. MacLean, A. E. Dementyev, and S. E. Barrett, Phys. Rev. B **77**, 214306 (2008).

[39] Y. Nishi, Jpn. J. Appl. Phys. **10**, 52 (1971).

[40] P. J. Caplan, E. H. Poindexter, B. E. Deal, and R. R. Razouk, J. Appl. Phys. **50**, 5847 (1979).

[41] A. Abragam, *Principles of Nuclear Magnetism* (Oxford University Press, 1983), p. 144.

[42] S. F. J. Cox, V. Bouffard, and M. Goldman, J. Phys. C **6**, 100 (1973).

[43] M. Goldman, S. F. J. Cox, and V. Bouffard, J. Phys. C **7**, 2940 (1974).

[44] W. E. Blumberg, Phys. Rev. **119**, 79 (1960).

[45] I. J. Lowe and D. Tse, Phys. Rev. **166**, 279 (1968).

[46] G. M. van den Heuvel, C. T. C. Heyning, T. J. B. Swanenburg, and N. J. Poulis, Phys. Lett. A **27**, 38 (1968).

[47] W. T. Wenckeback, G. M. van der Heuvel, H. Hoogstraate, T. J. B. Swanenburg, and N. J. Poulis, Phys. Rev. Lett. **22**, 581 (1969).

[48] D. S. Wollan, Phys. Rev. B **13**, 3671 (1976).

[49] S. Tanaka and H. Y. Fan, Phys. Rev. **132**, 1516 (1963).